

EXOSKELETAL STRAIN: EVIDENCE FOR A TROT–GALLOP TRANSITION IN RAPIDLY RUNNING GHOST CRABS

R. BLICKHAN

Universität des Saarlandes, Zoologie, AG Nachtigall, D-6600 Saarbrücken, Germany

R. J. FULL and L. TING

*University of California at Berkeley, Department of Integrative Biology, Berkeley,
CA 94720, USA*

Accepted 5 February 1993

Summary

Equivalent gaits may be present in pedestrians that differ greatly in leg number, leg design and skeletal type. Previous studies on ghost crabs found that the transition from a slow to a fast run may resemble the change from a trot to a gallop in quadrupedal mammals. One indication of the trot–gallop gait change in quadrupedal mammals is a distinct alteration in bone strain. To test the hypothesis that ghost crabs (*Ocypode quadrata*) change from a trot to a gallop, we measured *in vivo* strains of the meropodite of the second trailing leg with miniature strain gauges. Exoskeletal strains changed significantly (increased fivefold) during treadmill locomotion at the proposed trot–gallop transition. Maximum strains attained during galloping and jumping (1000×10^{-6} – 3000×10^{-6}) were similar to the values reported for mammals. Comparison of the maximum load possible on the leg segment (caused by muscular tension) with the strength of the segment under axial loading revealed a safety factor of 2.7, which is similar to values measured for jumping and running mammals. Equivalent gaits may result from similarities in the operation of pedestrian locomotory systems.

Introduction

Animals change gaits very much like we change gears when driving wheeled vehicles. Each gait transition is marked by an abrupt change in the speed-dependency of at least one variable characterizing the kinematics, energetics or the skeletal strain of the locomotory system (Alexander, 1988; Biewener and Taylor, 1986; Taylor, 1978). Most commonly, kinematic variables are used to characterize gait changes. During slow locomotion, humans use a walking gait, whereas at higher speeds they run. This transition from a walking to a running gait can be observed in most mammals. Running in mammals is generally distinguished from walking by at least two kinematic variables: (1) the occurrence of flight or aerial phases and (2) the pattern of leg movements.

It is difficult, if not impossible, to use kinematics alone to compare gaits among diverse species. This is especially true for animals that differ in leg number and use wave or

Key words: strain, locomotion, gait, exoskeleton, crustaceans, *Ocypode quadrata*, crab.

metachronal gaits. Arthropods using six legs have been described by some authors to have over 600 gaits, each resulting from a shift in phase among legs (Song, 1984). In contrast, other authors have stated that arthropods have one or at most two gaits: one slow and one fast (Hughes, 1952). Because the traditional definition of running includes an aerial phase, it was believed until recently that most arthropods could only walk. Only two species of arthropods have been shown to have aerial phases during high-speed locomotion: ghost crabs (Blickhan and Full, 1987; Burrows and Hoyle, 1973) and the American cockroach (Full and Tu, 1991).

We believe that an analysis of dynamics (i.e. kinetics in addition to kinematics) must be used to redefine gaits and to provide a more complete characterization of a walk and run (Blickhan, 1989a; Cavagna *et al.* 1977; Full, 1989). For example a stiff-legged walk is characterized by exchange of potential and kinetic energy as observed in a pendulum. During running, kinetic and potential energy fluctuate in phase as the body bounces on springy legs (Blickhan, 1989a,b; Cavagna *et al.* 1977). Blickhan and Full (1987) were the first to report that pendulum and bouncing gaits are not restricted to mammalian morphologies. Eight-legged ghost crabs use a pendulum-like energy-exchange mechanism at low speeds. Exchange between kinetic and potential energy can reach 55%. Crab dynamics clearly shows a transition from walking to running as does mammalian dynamics (Blickhan and Full, 1987). Ghost crab running is characterized by bouncing mechanics where kinetic and potential energy fluctuate in phase. Using this definition, Blickhan and Full (1987) showed that ghost crabs used a slow run which contains no aerial phases. In addition to identifying a slow running gait in ghost crabs, Blickhan and Full (1987) also described fast runs. As crabs switch from a slow to a fast run, they show a distinct change in the dependence of stride frequency on speed. Stride frequency increases linearly with speed during a slow run but becomes independent of speed during a fast run. Crabs increase speed during fast running by taking longer strides. It is well known that when mammals switch from a trot to a gallop, there is a distinct change in the dependence of stride frequency on speed. Stride frequency increases linearly with speed during a trot and becomes independent of speed during a gallop (Heglund *et al.* 1974; Heglund and Taylor, 1988). This pattern is not just qualitatively similar to that of ghost crabs: the transition in ghost crabs from a slow to a fast run occurs at exactly the speed and frequency predicted for a change from a trot to a gallop in mammals of similar mass, such as the mouse (Blickhan and Full, 1987).

The change from trotting to galloping at high speeds in quadrupeds is also characterised by a change in symmetry of the overall kinematics (Hildebrand, 1980). During mammalian trotting, hindlegs and front legs are placed on the ground simultaneously and all legs have about the same duty factor. The footfall pattern is evenly distributed in time and the gait is referred to as being symmetrical (Hildebrand, 1980). During a rotary gallop, front legs and hindlegs operate asynchronously and the gait is asymmetrical. Ghost crabs use a symmetrical gait analogous to a trot (Blickhan and Full, 1987). At very high speeds, a change in the stepping pattern has been described (Burrows and Hoyle, 1973). The two rear sets of legs are held off the ground and do not participate in locomotion. This sprinting is powered by alternate thrusts of two legs on the trailing side, with the leading legs serving as a passive skid. Blickhan and Full (1987), however,

were unable to find a consistent stepping pattern that uniquely characterized a gallop in the ghost crab. Apart from the differences in kinematics, the data as a whole suggest that equivalent gaits exist in species that differ greatly in form and that ghost crabs may trot and gallop.

One of the most recently investigated changes that characterizes the trot–gallop transition in mammals is an alteration in bone strain (Biewener, 1990). A redistribution of skeletal load caused by a change in muscular recruitment can also be used as an indicator of a gait transition. In trotting mammals, leading and trailing legs first decelerate and then accelerate the body during ground contact (Cavagna *et al.* 1977). During galloping in small mammals, the front legs decelerate the body, whereas the hindlegs provide acceleration. Determinants of bone strain provide further support for a redistribution of skeletal load at the trot–gallop transition. Skeletal strain changes dramatically at the trot–gallop transition in horses (Biewener, 1983; Biewener *et al.* 1988; Rubin and Lanyon, 1982), dogs (Rubin and Lanyon, 1982) and goats (Biewener and Taylor, 1986). Even though ghost crabs show a shift in leg loading and ground reaction force pattern similar to that found in mammals (Blickhan and Full, 1987), no comparable measurements of exoskeletal strain have ever been attempted for a fast-moving arthropod (Blickhan and Barth, 1985).

Previous results from the study of ghost crabs and cockroaches indicate that equivalent gaits may exist in animals that differ greatly in morphology (Blickhan and Full, 1987; Full, 1989). If equivalent gaits exist among legged animals, then we hypothesize that strain in the exoskeleton should change at the speed where stride frequency becomes independent of speed.

Materials and methods

Animals

Ghost crabs (*Ocypode quadrata* Fabricius) captured in the wild (Duke University Marine Laboratory, Beaufort, NC, USA) were housed at 25°C in individual containers filled with 50% sea water to a depth of less than 1cm and were fed fresh fish every second day.

Intermediate-sized ghost crabs tended to be the most cooperative runners, whereas the largest crabs tended to fight when prodded (Burrows and Hoyle, 1973; Blickhan and Full, 1987). However, large crabs have a more rigid exoskeleton and a larger leg surface which facilitates gauge placement and strain measurements. As a compromise, we selected the largest animals which would still run at high speeds ($N=5$; mass 10–16g; carapace width 25–30mm; Fig. 1; see Burrows and Hoyle, 1973).

Muscle force estimates

In the size range studied, scaling of carapace width, leg length and meropodite length were not geometric. Scaling exponents were less than 0.33. In particular, meropodite length became relatively shorter in larger animals ($P<0.0001$; Fig. 1). Nevertheless, carapace width can be used to estimate meropodite length [meropodite length (mm) =

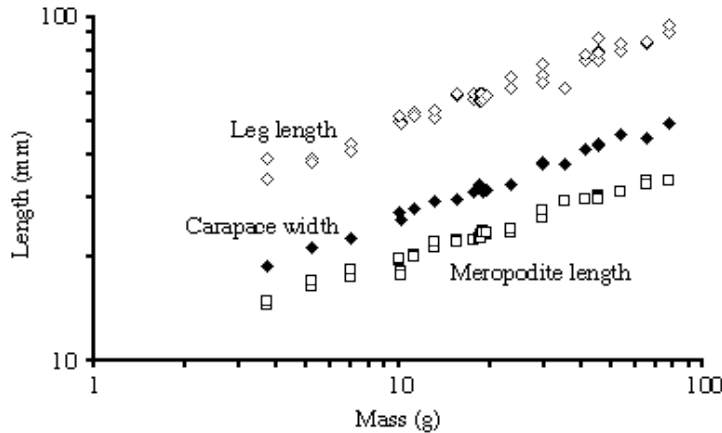


Fig. 1. Scaling of ghost crab carapace width (filled diamonds), length of second leg (open diamonds) and meropodite length (squares). \log carapace width = $(0.313 \pm 0.007) \log$ mass + (1.103 ± 0.010) ($N=46$); \log second leg length = $(0.306 \pm 0.009) \log$ mass + (1.382 ± 0.013) ($N=45$); \log second meropodite length = $(0.279 \pm 0.006) \log$ mass + (1.016 ± 0.008) ($N=45$); Dimensions: mass (g), length (mm). Values are given as mean \pm s.d.

$3.02 + 0.63$ carapace width (mm); $r=0.99$, $N=23$ crabs for left and right second leg for a total of 45 legs].

Loading of the meropodite is dominated by the flexor carpopodite and the extensor carpopodite muscles (Fig. 2). Extensor and flexor muscles are doubly pinnate and arranged one behind the other within the segment. Extensor muscles are located in the rostral aspect of the segment (i.e. relative to the body), whereas flexors are found caudally. Both muscles attach to reinforced dorsal and ventral ridges of the segment. Frozen legs were used to determine muscle fibre length and the angle of superficial fibre pinnation (Fig. 2A). We measured these with a protractor and caliper under a dissecting microscope. Muscle mass depended on the length of the meropodite, regardless of the leg examined (analysis of covariance). The cross-sectional areas of the respective muscles in the meropodite were obtained by dividing muscle volume (density assumed to be 1060 kg m^{-3}) by the average fibre length. From estimates of muscle stress (approximately 200 kPa; Perry *et al.* 1988) and the average angle of pinnation, we calculated the force pulling at the apodeme. On the basis of joint geometry, the maximum muscle + apodeme length change was 25%.

The estimated forces increased with meropodite length (Fig. 2B; four crabs, eight preparations of one muscle per leg from the first to the third pair). The force per body weight (\pm s.d.) calculated for the flexors (13.1 ± 1.1) and extensors (14.8 ± 2.6) of both the second and third leg did not differ significantly ($P > 0.2$). During fast locomotion, the extensors of the trailing legs generate the propulsive force. From the acting lever arms and the arrangement of the tendons it can be deduced that the resulting joint force is oriented roughly parallel to the long axis of the meropodite in this situation.

Strain measurements

To register the strains in the exoskeleton of crabs, miniature strain gauges (FLE-1-11,

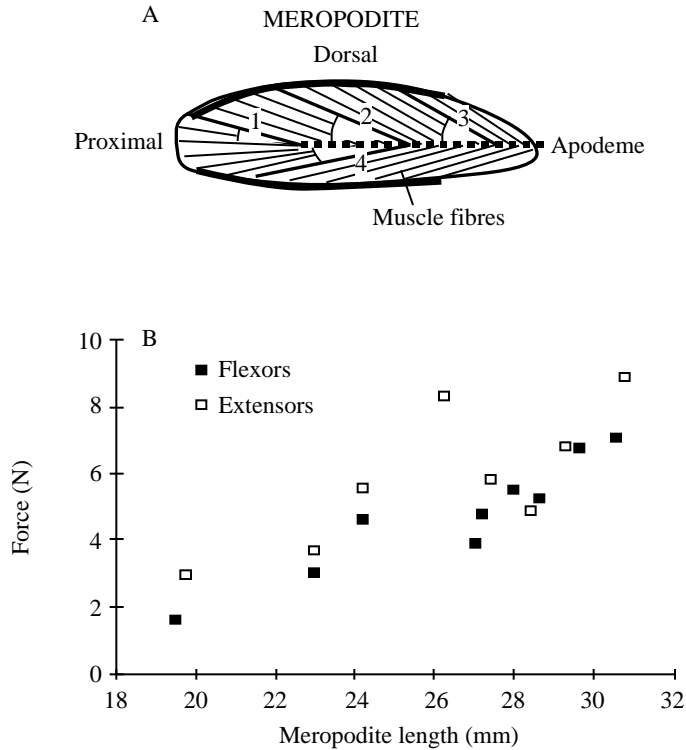


Fig. 2. Ghost crab muscle force estimates. (A) Arrangement of the extensor carpopodite muscle within the meropodite segment of the leg. The bold outline represents sites of muscular attachment. The numbered bold fibres (1–4) were measured to estimate fibre angle (α_i ; $i=1-4$) and fibre length at rest (l_i). Average length of flexor carpopodite fibres/length of meropodite = 0.379 ± 0.103 mm; average fibre angle of flexor carpopodite = $24.2 \pm 6.1^\circ$; $N=8$; average length of extensor carpopodite fibres/length of meropodite = 0.323 ± 0.033 ; average fibre angle of extensor carpopodite = $26.7 \pm 3.69^\circ$; $N=7$. Values are mean \pm s.d. (B) Calculated maximum muscle forces as a function of meropodite length.

TML, Tokyo Sokki Kenkyujo Co.) were attached to the exoskeleton (see Blickhan and Barth, 1985). Strain gauge rosettes which would allow the calculation of principal strain values were not used. The Young's modulus of the strain gauge (approximately 5×10^9 Pa, Glücklich, 1976) is at least of the same magnitude as that of the cuticle (approximately 3×10^8 Pa, Hepburn and Joffe, 1976), and the thickness of the cuticle (approximately $220 \mu\text{m}$) is only three times that of the strain gauge (total $70 \mu\text{m}$, backing $30 \mu\text{m}$; foil $5 \mu\text{m}$), so even a single gauge causes a significant local reinforcement. If the strains are largely determined by local bending of the exoskeleton, local stiffening and a shift of the neutral plane may result in strain readings of only one-fifth of the values occurring in the undisturbed cuticle (Glücklich, 1976; R. J. Full, unpublished results). Sufficiently small rosette gauges consist of a sandwich of three gauges on top of each other and are much stiffer. The large variation in the measured strain values rendered it impossible to calculate principal stress from the readings of single gauges attached in

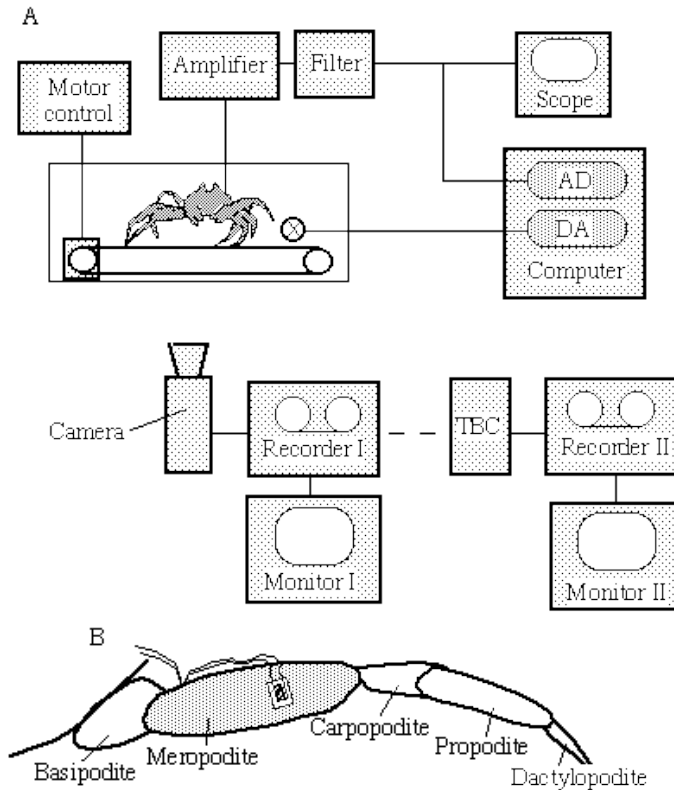


Fig. 3. Experimental arrangement for strain measurements during treadmill locomotion. (A) Strain signals were amplified and filtered before collection by an analogue-to-digital converter (AD). The start of strain data sampling was signalled by turning on an LED (circle with X) using the digital-to-analogue port (DA) of the converter. Trials were videotaped and later down-loaded with a time base corrector (TBC) to a VHS format for analysis. (B) Diagram showing the location and orientation of the strain gauge (base 5mm \times 2.5mm; grid 1mm \times 1.3mm) on the meropodite.

various directions. Thus, the observed changes in strain values can be caused by a change in orientation of principal stress (see Discussion) or by a change in the magnitude of skeletal loads. The second leg was selected because this leg is used during walking and running at high speeds (Blickhan and Full, 1987). The meropodite was chosen because it is the largest segment and has a smooth surface, which facilitates gauge application.

Strain gauges were applied to the leg in a cold room. The low temperature (4°C) served as a sufficient anaesthetic. To ensure adhesion, the thin wax layer of the leg was scraped off using sandpaper (grid number 220 TS). A small drop of sticky wax (Kerr) was used to secure the wires of the gauge to the leg. This anchoring point allowed precise gauge orientation. The gauge was fixed to the anterior side of meropodite with a small droplet of fast-setting adhesive (cyanoacrylate) five-eighths of the way down the meropodite. The gauge was oriented dorsoventrally within $\pm 7^\circ$ (Fig. 3B).

Teflon-insulated copper wires were soldered to the gauge leads and secured proximally

at the meropodite and to the lateral edge of the carapace with droplets of wax. A loop of wire was formed to ensure mobility of the leg. The wires were soldered to a miniature plug previously affixed to the carapace with adhesive. During the experiments, the wires leading to the animal were slack enough to allow free motion on the treadmill.

The strain gauge was connected *via* the plug on the carapace to a Wheatstone bridge contained in an amplifier and supply unit (see Fig. 3; System 2100, Vishay). The filtered (two-pole Butterworth filter) strain data were digitized ($1000\text{ samples s}^{-1}$ for 4s; NBNIO16 A/D Board, National Instruments) on line and stored on the hard disk of a personal computer (software, LabView, National Instruments; computer, Macintosh IIfx, Apple). Synchronization between film and strain data was provided by switching on an LED at the start of sampling using the DA port of the converter board.

Kinematics

Strain measurements were collected from animals moving on a variable-speed treadmill (track length 0.4m; width 0.15m; maximum speed 2 ms^{-1}). Treadmill speed was measured by tracking markers on the belt with a high-speed video camera.

To judge the quality of the trials and to measure stride frequency and contact time, we recorded the animal's movement with a high-speed video system at 250 frames s^{-1} (Ektapro SE, Kodak). A mirror placed behind the track allowed us to observe the animal's position on the track. Data were then copied after timebase correction (AE 61, Hotronic) to a VHS recorder (6300, Panasonic), which allowed easy frame-by-frame analysis. Trials were judged to be acceptable if the crab kept pace with the tread belt, ran freely and the strain pattern was regular.

Experimental protocol

After application of the strain gauges in the cold room, the leads on the animal were soldered to the suspended wires attached to the bridge and amplifier. The animals were allowed a minimum of 30min to recover, so that their body temperature equalled room temperature (24°C). In each trial, the treadmill belt speed was increased to the desired sustainable speed, then the camera and recorder system were started and the strain signal was sampled by the computer. Fast runs were obtained first. Slower trials were obtained after a 5–10min recovery period. After several trials, the animals were allowed to rest in sea water before acquisition of further data. Animals were tested only once a day.

Buckling tests

Strain recordings under defined loading conditions along with maximal buckling load tests were obtained by loading the meropodites axially with a materials testing machine (1122 Instron; 500N tension load cell 2511-111). Legs of freshly killed crabs ($N=5$; legs 1–4 left and right side for each) were ablated at the coxae and then trimmed, leaving the joints of the meropodite intact. Leg segments were then placed within a compression rig (compression cage 1122) used for the Instron machine. A layer of sandpaper prevented slippage. These leg segments were loaded at a constant speed of 5 mm min^{-1} ,

corresponding to a strain rate of about $0.25 \text{ strain min}^{-1}$, which is about a factor of 10 lower than the maximum rates measured in the exoskeleton during jumping and corresponds to the average loading rate during trotting. The hysteresis loops are expected to change only little for different frequencies within an order of magnitude (Blickhan, 1986). The extent of displacement was controlled manually. In the first set of trials, legs were loaded cyclically with constant displacement (1.3mm). In the case of high forces, legs were loaded up to the maximum force that could be generated by the muscles (approximately 5N). In a second set of trials, the legs were loaded until buckling occurred.

Results

Kinematics

Stride frequency (f) increased linearly with speed (U) during walking (to 25 cm s^{-1}) and trotting, but became independent of speed at approximately 60 cm s^{-1} and a stride frequency of 8 s^{-1} (Fig. 4A). Stride length (l_s) increased linearly with speed, reaching 16cm at the highest speeds (Fig. 4B). Stride length did not depend on speed during walking. Contact duration (the length of time a leg is on the ground during a stride) decreased hyperbolically from 0.4s during slow walks to less than 50ms at the highest speeds (Fig. 4C). During walking, the duty factor (the ratio of contact duration to stride period) varied between 0.4 and 0.9 (Fig. 4D). The duty factor did not change significantly with speed above 20 cm s^{-1} ($r=0.30$, $N=33$, $P>0.05$).

Strain measurements

Strain measurements reflecting the cyclic loading of the second leg were readily discernable at all speeds (Fig. 5). During running (i.e. trotting and galloping), the beginning of ground contact caused a distinct rapid increase in the strain. Strain began to decline in a characteristic 'shoulder' before the end of ground contact. In galloping and jumping animals, the strain level during ground contact increased significantly compared with values recorded during walking and running. These high strain values represented tensile strain probably caused by bending and/or bulging at the site of measurement. This was verified by simple three-point lateral bending and dorsoventral compression of the segment (see below). Highest strain values were recorded from jumping animals, but comparable magnitudes were frequently reached by fast-running animals, indicating similarities in leg loading for the two activities.

Peak strain increased linearly with speed for each animal up to a speed of 60 cm s^{-1} (Fig. 6A). At higher speeds, strain increased significantly by three- to sixfold ($P<0.001$; factor of 5.1 ± 1.3 , s.d.). The increase in strain with speed is best visualized by plotting peak strain values normalized to the average peak strains measured at speeds greater than 60 cm s^{-1} (Fig. 6B). The difference in peak strain below and above 60 cm s^{-1} (i.e. for a trot and a gallop) was apparent even within an individual record of an animal running at this transition speed (Fig. 7).

Variation in strain recordings from animal to animal was considerable. For example, two different animals moving at low speeds ($0\text{--}40 \text{ cm s}^{-1}$) had average peak strain values (\pm s.d.) that ranged from $45.2 \times 10^{-6} \pm 9.9 \times 10^{-6}$ to $255 \times 10^{-6} \pm 83 \times 10^{-6}$. At high speeds

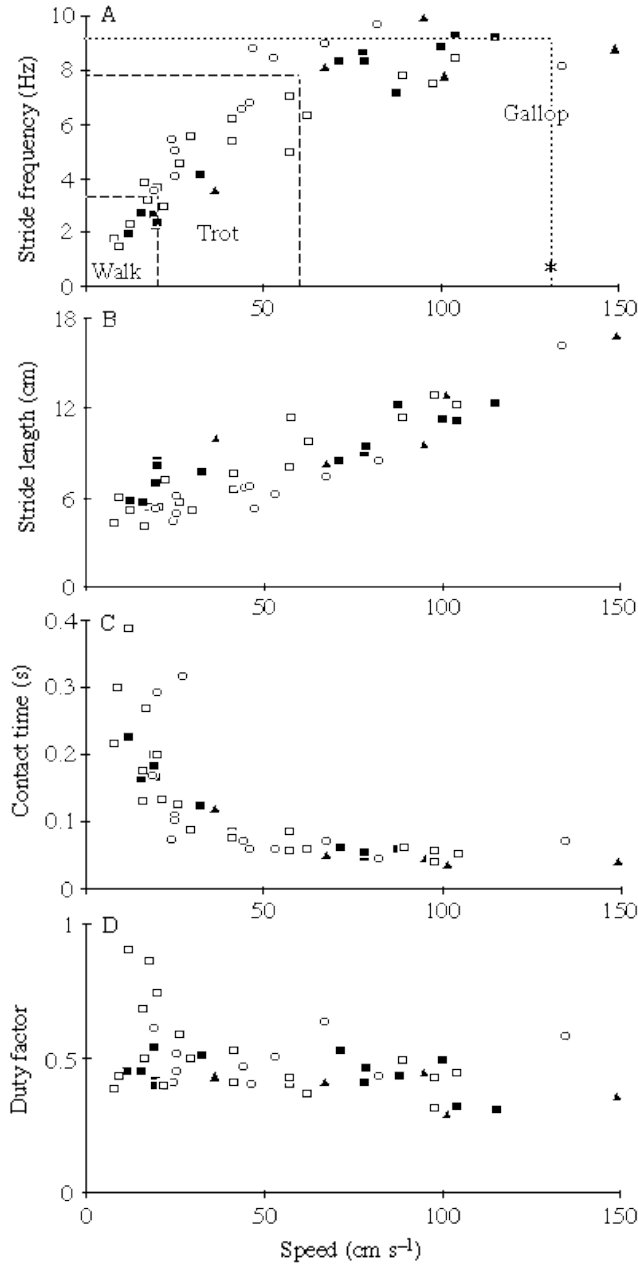


Fig. 4. Kinematic variables as a function of speed. (A) Stride frequency (f) became independent of speed (U) at high running velocities. Speed and frequencies of gait transitions (dashed lines) were derived from scaling relationships obtained for quadrupedal mammals (Heglund and Taylor, 1988). Regressions (\pm s.e.): $f = (7.02 \pm 2.10)U + (2.72 \pm 0.86)$, $r = 0.67$ for $0.2 \text{ ms}^{-1} < U < 0.6 \text{ ms}^{-1}$; $f = (0.25 \pm 0.89)U + (8.26 \pm 0.87)$, $r = 0.071$ for $U > 0.62 \text{ m s}^{-1}$. (B) Stride length increased linearly with speed [$l_s = (0.076 \pm 0.005)U + (0.042 \pm 0.004)$, $r = 0.95$]. (C) Contact time decreased hyperbolically with speed. (D) The duty factor (contact time/stride duration) was about 0.5 over the entire speed range. Only at speeds below 20 cm s^{-1} were high duty factors typical for walking found. Symbols represent different individuals. Values are given as mean \pm s.e.m. The asterisk marks the preferred galloping speed.

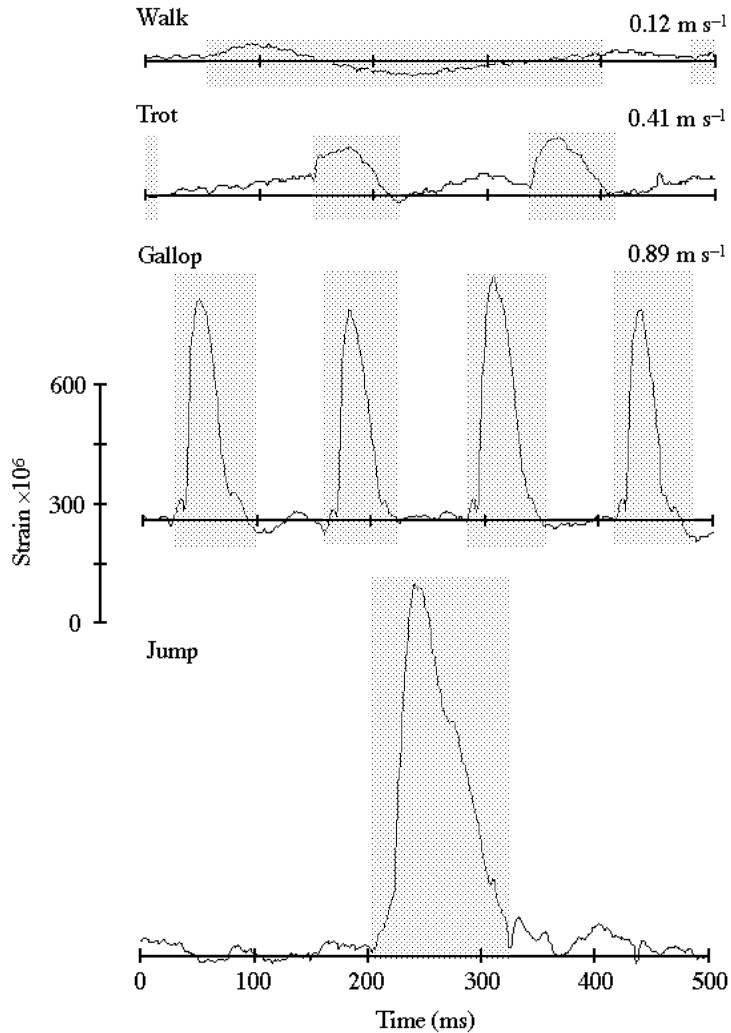


Fig. 5. Strain recordings during various activities. The stippled pattern represents ground contact. During walking, strain readings varied periodically. Both tension and compression occurred during ground contact. During slow runs (trotting), increased levels of strain were measured during the shorter ground contact time. Fast runs were characterized by the occurrence of high strain values which were only surpassed during jumps.

(>70 cm s⁻¹) the values ranged from $198 \times 10^{-6} \pm 1 \times 10^{-6}$ to $1610 \times 10^{-6} \pm 780 \times 10^{-6}$ with a total average of $711 \times 10^{-6} \pm 377 \times 10^{-6}$ for five animals. Variation in peak strain was substantial even for the same animal (s.d.=50% of mean) and best demonstrated the variability in leg loading. The maximum strain values observed in three animals during galloping ranged from 1000×10^{-6} to 2400×10^{-6} and during jumping from 1600×10^{-6} to 3000×10^{-6} .

Buckling strength

Under axial loading of the meropodite, hystereses were observed with respect to both

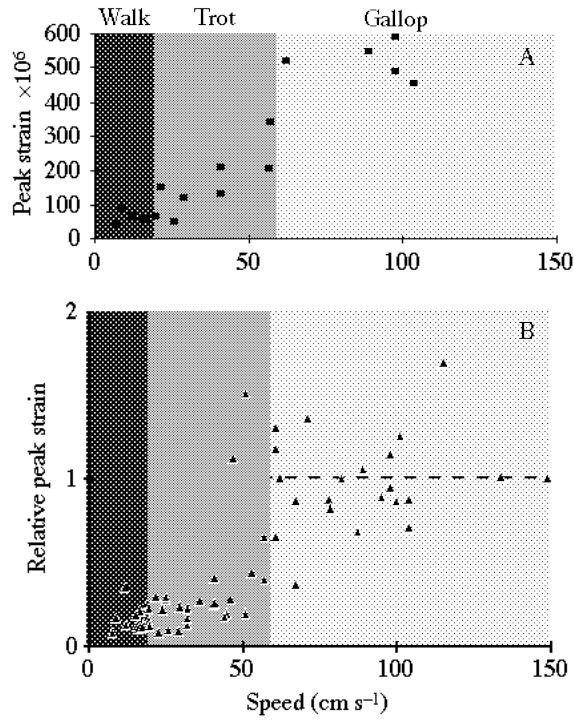


Fig. 6. Peak strain in ghost crabs as a function of speed. (A) Peak strains as a function of speed for an individual. (B) Peak strain values normalized to their average value (five crabs) above 60 cm s⁻¹. Strain increased at this speed to a much higher value, indicating a change in the loading of the second leg and a gait transition.

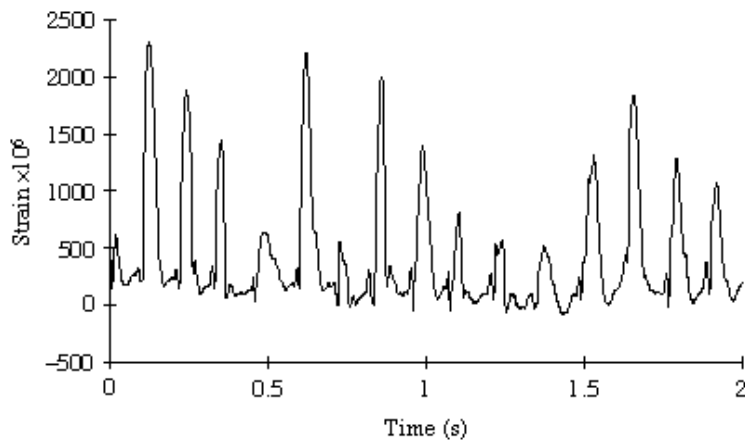


Fig. 7. Exoskeletal strain of a ghost crab running at the transition from a trot to a gallop (60.5 cm s⁻¹). Peak strains showed large fluctuations and varied between trotting and galloping patterns.

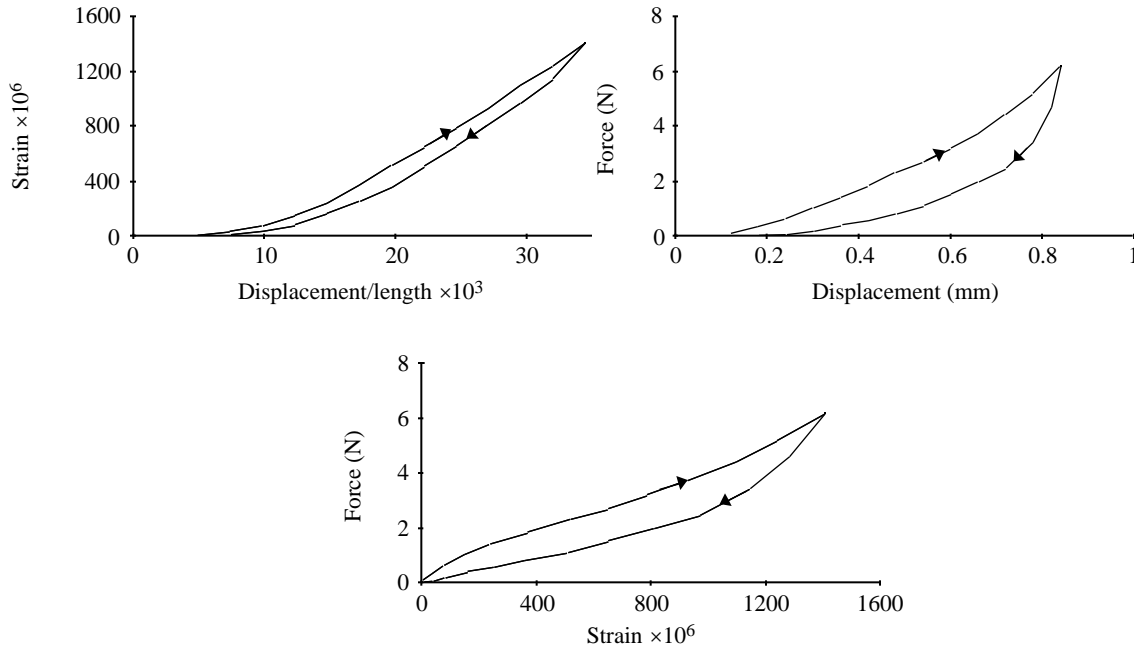


Fig. 8. Strain, displacement and force obtained during uniaxial testing of a ghost crab's meropodite. Loading rate was 5mmmin^{-1} . Neither force nor displacement was free of hysteresis when plotted against the measured strain.

displacement and force, indicating that viscous elements are not only in series but also in parallel with the gauge (Fig. 8). In other words, the cuticle itself showed viscoelastic behaviour at loading rates corresponding to values observed during locomotion at intermediate speeds. Strain recordings were strongly dependent upon the site of measurement along the leg axis. Despite the careful placement of the gauges (at 0.370 ± 0.028 segment lengths from the distal joint), small differences in the placement of the gauges may have been responsible for a large fraction of the differences in the strain values measured for different animals. Dorsoventral compression of the meropodite perpendicular to its long axis at various sites always resulted in tension because the cuticle was bulging. The muscles in the meropodite generate dorsoventral force components.

All meropodite segments investigated failed under axial loading by buckling, most frequently at about half meropodite length. For frozen specimens, the average maximal load-to-weight ratio for the first, second and third legs was 71 ± 11 (s.d.; 3 crabs; 17 legs) regardless of size. For a fresh specimen (31.1g), the ratio was considerably lower (40 ± 9 ; s.d.; 1 crab; 6 legs). The large standard deviation in the ratio of buckling strength of the left to the right leg (1.05 ± 0.36 ; s.d.; $N=10$) indicated considerable variability in strength even within a single individual. For a single animal, strength among comparable contralateral legs can differ by a factor of 1.7. The peak strain values attained in two specimens before buckling (600×10^{-6} and 2000×10^{-6}) were of the same order of magnitude as the maximum strains observed in running animals.

Discussion

Crabs walk, trot and gallop

Gait changes can be recognized by discontinuities in the speed dependency of mechanical or metabolic variables (Alexander, 1989). Ghost crabs change gait from an inverted pendulum-like stiff-legged walk to a bouncing or trotting gait (Blickhan and Full, 1987). The present results clearly show that a distinct alteration in exoskeletal strain took place at the hypothesized trot–gallop transition of crabs. The strain pattern shifted from a rounded maximum at a trot to a narrow peak during a gallop (Fig. 5). Strain increased by over fivefold at the transition speed (Fig. 6). Crabs running at the trot–gallop transition speed shifted from one pattern to the other (Fig. 7). Strain data in combination with leg kinematics strongly suggest a redistribution of exoskeletal load at the trot–gallop transition in ghost crabs. In mammals, however, bone strain is decreased, whereas in ghost crabs exoskeletal strains were increased.

Why crabs change from trotting to galloping

Large mammals switch from trotting to galloping to save energy, but crabs simply change gait to achieve a higher running speed. Switching gaits from a walk to a trot can be simply explained by the physical limitations of the inverted pendulum mechanism used during walking in many animals, including ghost crabs. The pendulum mechanism of energy exchange is limited to low speeds by the gravitational acceleration that drives the system (Blickhan and Full, 1987; Cavagna *et al.* 1977). At high speeds, large centrifugal forces will disrupt the body's path of near circular arcs and prevent energy exchange. Unlike the walk–trot transition, the trot–gallop transition may not have a single, simple physical reason that determines the gait change in all animals.

Energetic cost

Changing gait from a trot to a gallop can minimize the energetic cost of locomotion. As the trotting gait of a horse is extended to higher and higher speeds, the metabolic cost to trot a given distance (cost of transport) will eventually exceed that required for galloping at the same speed (Hoyt and Taylor, 1981). The increase in economy achieved by galloping in large mammals might be caused by the recruitment of the trunk as an additional spring (Alexander, 1988; Taylor, 1978).

The change in gait from a trot to a gallop in ghost crabs probably does not minimize metabolic energy cost. The minimum cost of locomotion is attained at a slow walk (Full and Prestwich, 1986). Trotting and galloping speeds exceed the speeds at which ghost crabs attain their maximal rate of oxygen consumption (Full, 1987). Speeds faster than a slow walk require energy from accelerated glycolysis and high-energy phosphates and are metabolically very expensive (Full and Weinstein, 1992). Even so, we cannot rule out the possibility that trotting at speeds higher than we observed would result in an even greater energy demand than if a gallop were used. Stride frequency does not continue to increase with speed during galloping (Fig. 4A), so that the cost associated with more rapid rates of muscle force production may be reduced.

Musculo-skeletal force reduction

A change in gait from a trot to a gallop may be triggered when musculo-skeletal forces reach a critical level (i.e. supporting the hypothesis of stress similarity). Farley and Taylor (1991) found that horses naturally change from a trot to a gallop at speeds that reduce peak forces on tendons, bones and muscle, but which also decrease the metabolic cost of transport. Horses carrying weights switch gait at lower speeds than horses carrying no additional load, but at the same critical level of force. In mammals, peak force exerted by limb extensors appears to increase within a trotting gait, but decrease upon transition to a gallop (Taylor, 1985). Force platform studies have shown a decrease in the peak vertical ground reaction force when mammals change from a fast trot to a slow gallop (Biewener, 1983; Cavagna *et al.* 1977; Heglund *et al.* 1982). For example, peak vertical force in dogs decreases from 2.5 times body weight to 1.5 times body weight.

There is no evidence for a reduction in peak force exerted by muscles at the trot–gallop transition in ghost crabs. Force platform studies failed to show a consistent decrease in peak vertical ground reaction force when crabs changed from a fast trot to a slow gallop (Blickhan and Full, 1987). These results are not conclusive, however, because no detailed indirect mechanical analysis of a crab's leg (i.e. based on ground reaction force and leg kinematics; Biewener, 1989) has been made to estimate muscle or exoskeletal stress.

Direct evidence that peak stresses in the musculo-skeletal system are associated with gait changes in mammals comes from the *in vivo* measurement of bone strain. Strain in goats (Biewener and Taylor, 1986), dogs (Rubin and Lanyon, 1982) and horses (Biewener, 1983; Biewener *et al.* 1988; Rubin and Lanyon, 1982) increases within a trotting gait, but decreases as these mammals change from a trot to a gallop. Strain levels at the trot–gallop transition are similar in goats, dogs and horses, despite differences in absolute speed (Biewener and Taylor, 1986).

Our direct measurements of exoskeletal strain in the ghost crab did not show a reduction at the trot–gallop transition (Fig. 6B). On the contrary, strain increased by over fivefold. Although further analyses of muscle and apodeme forces are required, it does not appear that ghost crabs change gait to reduce skeletal strain or stress. Strain in the skeleton of the ghost crab during a fast trot is far lower than in mammals moving at an equivalent speed. Trotting crabs can distribute the load among more than six legs, whereas during galloping propulsion is only provided by one or two trailing legs. In contrast, only the timing of the legs changes with the gait transition in quadrupeds.

Speed and the rate of muscle force production

A third reason why ghost crabs, and perhaps other small animals, change gait may simply be to run faster. Ghost crabs (Fig. 4A) and cockroaches (Full and Tu, 1990) reach near-maximal stride frequencies at the proposed trot–gallop transition. Faster speeds are attained by taking longer strides. Stride frequencies at the proposed trot–gallop transition can be extremely high. The American cockroach cycles its legs at 25Hz, the same as its wingbeat frequency during flight (Full and Tu, 1991). If insufficient time is available to relax muscles before their antagonists contract, then interference of propulsive power may result. Marsh and Bennett (1986) argued that speed may be limited at cold

temperatures in lizards for just such a reason. The estimated duration of the muscle's active state became nearly equal to half the stride period at low temperatures. The change from trotting to galloping may be a measure to increase speed by increasing stride length at near-maximal rates of force production.

Why does the strain increase at the trot–gallop transition?

In contrast to the strain reduction measured in quadrupedal mammals, strain in the ghost crab leg increased at the trot–gallop transition. Why does this occur, and does it reveal a fundamental difference between endoskeletons and exoskeletons?

The reduction in load on a leg can be achieved by increasing the contact duration and contact length (i.e. the time or distance over which a force is developed) or by increasing the number of legs that share the load. In dogs, a reduction in the peak ground reaction force during the transition to a gallop is possible because the contact duration during which each leg accelerates or decelerates during a step is increased (Cavagna *et al.* 1977). In other words, the compliance of each leg increases. This results in a larger angle of attack (the angle between the vertical and the leg at touchdown) and an increased contact length (Blickhan, 1989*a*). These changes can be facilitated by the bending and rotation of the trunk.

Measurements of single leg forces are not available for the ghost crab. Nevertheless, an increase in the ground reaction force for each leg of the crab would be consistent with the increase in strain measured (Fig. 6). Because stride frequency does not increase with speed (Fig. 4A), the momentum delivered to the ground by a leg must increase with speed. Furthermore, the number of legs generating this momentum decreases (Burrows and Hoyle, 1973). Contact durations clearly become shorter with increasing speed (Fig. 4C). These changes demand that the increase in momentum must be generated within a shorter period. A greater load on the leg during galloping is the consequence. However, as there is no discontinuous drop in the contact time at the trot–gallop transition other factors must contribute to the observed pattern.

Crabs cannot easily decrease the legs' angle of attack in order to increase contact duration. Because of their morphology, bending of the trunk is neither possible nor desirable. At low angles of attack, the dactylopodites of the crab's trailing legs are aligned nearly parallel to the substratum when they first touch down (Fig. 9). If the trailing legs decelerate the body, as is seen during fast trotting (and galloping in large mammals), then the chances of slipping would be increased or the dactylopodytes might dig deeply into the sand and hamper the animal's movement. The leading leg would have similar problems in the acceleration phase. Thus, the design of the crab's locomotory apparatus prohibits trotting or a similar loading of leading and trailing legs at high speeds. During galloping, the trailing legs accelerate, while the leading legs largely decelerate the body (Blickhan and Full, 1987). By using the leading legs simply as passive skids, active muscles in these legs are primarily stretched. Strain data (Fig. 10) suggest that, during galloping, forces generated in the leading legs are lower than those in the trailing legs. Less energy may be necessary to operate the leading legs. Because of the symmetry of the locomotory system, the crab has the unique option of turning and switching its leading and trailing legs. Thus, a decrease in energy necessary to drive the leading leg might

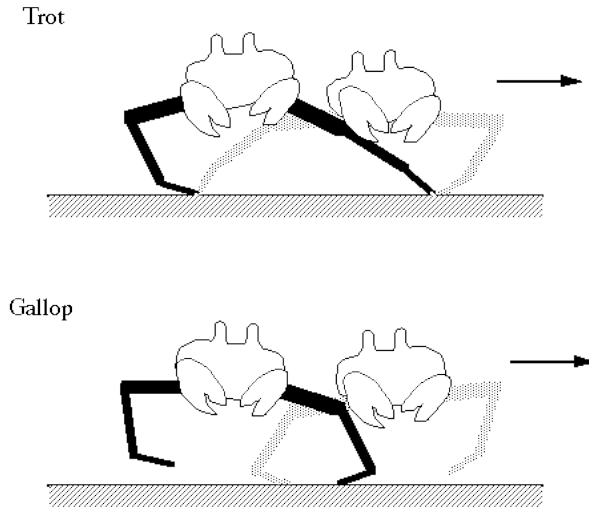


Fig. 9. Deceleration (black legs) and acceleration (stippled legs) during trotting and galloping in ghost crabs. In a trot, the flat angle of attack of the trailing leg during deceleration may make force transmission difficult. The chances of slipping would be increased or the dactylopodytes might dig deeply into the sand and hamper the animal's movement. The leading leg would have similar problems in the acceleration phase. During galloping, the trailing legs accelerate, while the leading legs largely decelerate the body (Blickhan and Full, 1987). By using the leading legs simply as passive skids, activated muscles in these legs are primarily stretched.

outweigh the increase in energy necessary to drive the trailing leg, since the animal could stave off fatigue by turning round. The tendency to turn round after exhausting runs can be observed in the laboratory as well as in animals roaming the beach in nature (Burrows and Hoyle, 1973).

The strategy of increasing the number of load-bearing legs or placing legs in a sequence that reduces the load on individual legs is not used by ghost crabs despite the larger number of legs available to them. Differences in leg length and overall size could be part of the reason for this. Because of the crab's sideways movement and leg arrangement, use of some legs during high-speed locomotion could disrupt stability. In particular, the fourth walking leg seems to be too short to be of any use during fast locomotion and is typically held in the air. Use of the fourth leg to reduce load on other legs would require counteraction from the chelipeds in order to prevent anterior-posterior yawing. Clearly, this is not an option for fast locomotion. A reduction in the number of load-bearing legs would increase the load on individual legs, but could ensure stability.

A further problem arising from using a greater number of legs during fast locomotion is an increased demand for precise control of each individual leg. Precise stepping does not appear to be characteristic of crustacean locomotion (Clarac, 1981). Ghost crabs demonstrate a surprising amount of variability in the phase relationships between the legs (Blickhan and Full, 1987). For example, in one experimental session the same individual moved its second leg in phase with the first leg in one trial and out of phase in the next

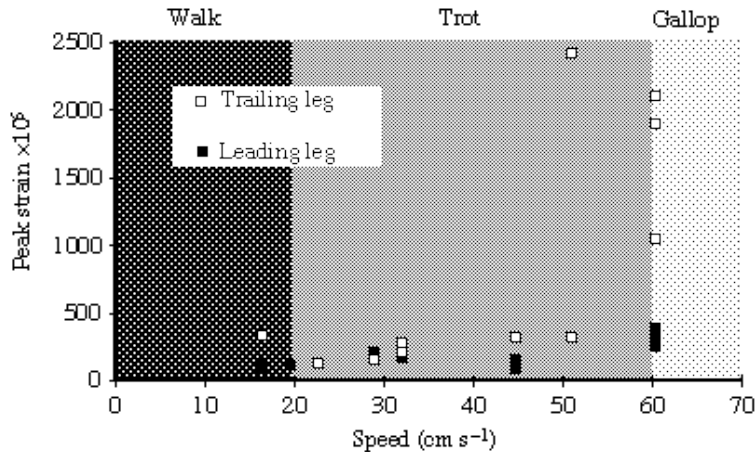


Fig. 10. Peak strain measured while the same individual ran in opposite directions and the site of measurement switched from the trailing to the leading side. In the transition region (60cm s^{-1}), the strains in the leading leg were low compared with the values recorded in the trailing leg.

trial. A reduction in the number of load-bearing legs increases the load on individual legs, but could simplify control.

One might reason that many-legged animals should use all of their legs to run faster and increase power output. A closer look reveals, however, that using fewer legs at higher speeds is a very common strategy. Recent experiments have shown that cockroaches switch from hexapedal to quadrupedal, and even to bipedal, locomotion with increasing speed (Full and Tu, 1991). Similar transitions have been observed in lower vertebrates. Lizards switch from a trot to a fast run (R. Blickhan and R. L. Marsh, in preparation) with increasing speed and can become bipedal (Snyder, 1962). Ghost crabs, cockroaches and lizards use only their longest legs during fast locomotion. Longer legs can increase contact length or, for a given speed, contact duration. Using fewer legs will result in a greater force per leg, but using longer legs will increase contact duration and decrease the rate of operation of the musculature. Quadrupedal galloping and the reduction of load at the trot–gallop transition may be unique to the special body plan of cursorial mammals and aid in sustaining high speeds aerobically.

In conclusion, the increase in strain at the trot–gallop transition is not caused by the mechanical differences between exoskeletons and endoskeletons *per se* but to differences in the design and control of the locomotory system. Such differences are (a) a larger number of legs, (b) unequal leg lengths, (c) spike-like ‘feet’ combined with the different mechanics of the leading and trailing legs, and (d) the limited time for locomotor control.

Strain and strength in exoskeletons and endoskeletons

The conservative properties of bone as a material and its operation at similar safety factors mean that peak strains measured in mammals are relatively independent of size and type of activity (Lanyon and Rubin, 1985). No comparable statement can be made for the exoskeleton of arthropods. The only published strain measurements on leg segments

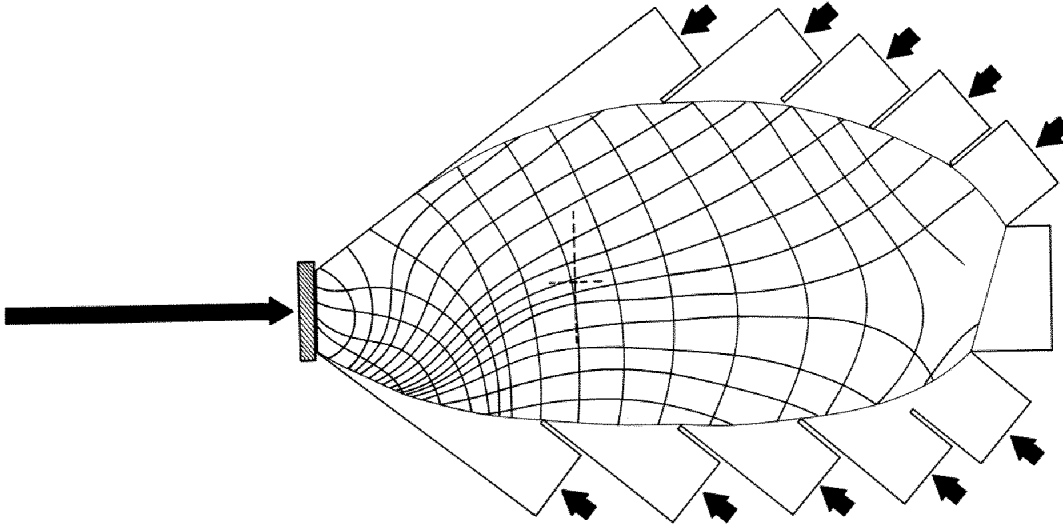


Fig. 11. Lines of principal stress in a photoelastic model of the meropodite. The leg segment is modelled as a disc (PS-1A) loaded by a joint force distally (long arrow on the left) and distributed muscular forces (short arrows) at the dorsal and ventral rim. The dashed cross marks the orientation of the strain gauge in the experiments. The hatched area shows the rubber sheet simulating reinforcements of the joint.

of arthropods indicate that during locomotion much lower strain values occur in these animals than in mammalian skeletons (Blickhan and Barth, 1985). However, these data were collected in spiders during slow walking, not during sprinting or jumping.

Surprisingly, even though strain in the ghost crab's exoskeleton increased at the trot-gallop transition, maximal strain values were similar to values observed for long bones of running and jumping mammals (2000×10^{-6} – 3000×10^{-6} ; Biewener, 1990; Lanyon and Rubin, 1985). Peak strain values on the meropodites of the ghost crab during fast locomotion reached values of 1000×10^{-6} in many individuals. The highest values measured were during galloping (2400×10^{-6}) and jumping (3000×10^{-6}). These results indicate that the maximum deformability of the arthropod exoskeleton may be similar to that of the vertebrate endoskeleton. If average peak strain values reached during galloping are considered ($711 \times 10^{-6} \pm 377 \times 10^{-6}$; s.d.; $N=5$), leg segments in arthropods may be even stiffer than in vertebrates, despite the exoskeleton's thin-walled construction. Any conclusion, however, concerning low strain values and the high stiffness of the exoskeleton should be considered tentative. To avoid stiffening of the crabs' thin cuticle, rosette strain gauges could not be applied and the principal strain axes could not be determined. Gauges aligned further away from the principal axes could have underestimated the strain values by larger amounts. Moreover, any change in the peak values of the strain could have been induced by a change in the direction of the principal strains. Our preliminary photoelastic simulations on discs shaped like meropodites (Fig. 11) show that the principal strain axes are oriented almost parallel to the main axis of the segment in the investigated region. However, these results must be treated with

caution because bending and bulging, which are important in the actual leg, were not simulated in the model experiments.

Similarities in peak strain for bone and exoskeleton during locomotion raise the question of whether or not the ghost crab's exoskeleton is also operating with a safety factor comparable to those estimated for mammals. Comparative studies of the strength of long bones under a bending load have revealed a safety factor of about two for jumping kangaroo-rats, and running dogs and horses (Biewener, 1989). Under axial loading, meropodite segments of the ghost crab failed by buckling, as is to be expected for thin-walled tubes. Buckling is probably the mode of failure when a crab's leg is subjected to bending, as during locomotion. Because of the natural bend in the segment, loading in a test machine is not purely axial, and failure by buckling and bending can be considered to be relatively equivalent (Currey, 1967; Blickhan, 1986). The meropodite was able to withstand weight-specific loads up to 40. On the basis of the morphology of the doubly pinnate muscles, a maximum weight-specific axial joint force of 14.8 was estimated (see Materials and methods). A safety factor of about 2.7 results from the ratio of maximum muscle force to segment strength. On the one hand, this estimate may be high because ground impact and dynamic forces were not considered. On the other hand, axial loading in the test machine neglects the stabilizing action of the muscle force component perpendicular to the long axis of the segment and the possibility that hydrostatic forces increase strength. Whatever the actual safety factor, buckling perpendicular to the long axis seems to be the most common mode of failure in nature, as can be seen from injuries. Injuries are very frequent and many crabs may have to cope with even lower safety factors over a period of several days or weeks because of these injuries.

Given the differences in material, shape and mode of failure and the possibilities of repair, the similarity of strain values and safety factors in the skeleton of crabs and mammals is surprising. The strain pattern found in the present study adds further evidence to the suggestion that ghost crabs indeed change gait from a walk, to a trot, to a gallop at speeds and frequencies similar to those of mammals of the same body mass. The modes of operation of legged systems may be limited and may require similar skeletal stiffness. General musculo-skeletal problems may be solved by common structural solutions using different structural arrangements. However, more of these general rules of construction await discovery.

R.B. is grateful to all members of the PolyPEDAL Laboratory at U.C. Berkeley for enthusiastic support. R. Weinstein's skill in programming LabView facilitated this project considerably. Special thanks are due to M. Koehl for taking the risk and allowing us to use the Instron Testing Machine. This research was supported by NSF Grant Physiological Processes DCB 89-04586 and by a DFG travelling grant (BI 236-3).

References

- ALEXANDER, R. MCN. (1988). Why mammals gallop. *Am. Zool.* **28**, 237-245.
ALEXANDER, R. MCN. (1989). Optimization of gaits in the locomotion of vertebrates. *Physiol. Rev.* **69**, 1199-1227.

- BIEWENER, A. A. (1983). Allometry of quadrupedal locomotion: the scaling of duty factor, bone curvature and limb orientation to body size. *J. exp. Biol.* **105**, 147–171.
- BIEWENER, A. A. (1989). Mammalian terrestrial locomotion and size. *BioScience* **39**, 776–783.
- BIEWENER, A. A. (1990). Biomechanics of mammalian terrestrial locomotion. *Science* **250**, 1097–1103.
- BIEWENER, A. A. AND TAYLOR, C. R. (1986). Bone strain: a determinant of gait and speed? *J. exp. Biol.* **123**, 383–400.
- BIEWENER, A. A., THOMASON, J. AND LANYON, L. E. (1988). Mechanics of locomotion and jumping in the horse (*Equus*): *in vivo* stress in the tibia and metatarsus. *J. Zool., Lond.* **214**, 547–565.
- BLICKHAN, R. (1986). Stiffness of an arthropod leg joint. *J. Biomech.* **19**, 375–384.
- BLICKHAN, R. (1989a). The spring-mass model for running and hopping. *J. Biomech.* **22**, 1217–1227.
- BLICKHAN, R. (1989b). Running and hopping. In *Energy Transformations in Cells and Organisms* (ed. W. Wieser and E. Gnaiger), pp. 183–190. Stuttgart: Thieme.
- BLICKHAN, R. AND BARTH, F. G. (1985). Strains in the exoskeleton of spiders. *J. comp. Physiol.* **157**, 115–147.
- BLICKHAN, R. AND FULL, R. J. (1987). Locomotion energetics of the ghost crab. II. Mechanics of the centre of mass during walking and running. *J. exp. Biol.* **130**, 155–174.
- BURROWS, M. AND HOYLE, G. (1973). The mechanism of rapid running in the ghost crab, *Ocypode ceratophthalma*. *J. exp. Biol.* **58**, 327–349.
- CAVAGNA, G. A., HEGLUND, N. C. AND TAYLOR, C. R. (1977). Mechanical work in terrestrial locomotion: two basic mechanisms for minimizing energy expenditure. *Am. J. Physiol.* **233**, R243–R261.
- CLARAC, F. (1981). Decapod crustacean leg coordination during walking. In *Energetics and Locomotion in Arthropods* (ed. C. F. Herreid and C. R. Fournier), pp. 31–72. New York: Plenum Press.
- CURREY, J. D. (1967). The failure of exoskeletons and endoskeletons. *J. Morph.* **123**, 1–16.
- FARLEY, C. T. AND TAYLOR, C. R. (1991). A mechanical trigger for the trot–gallop transition in horses. *Science* **253**, 306–308.
- FULL, R. J. (1987). Locomotion energetics of the ghost crab. I. Metabolic cost and endurance. *J. exp. Biol.* **130**, 137–153.
- FULL, R. J. (1989). Mechanics and energetics of terrestrial locomotion: From bipeds to polypeds. In *Energy Transformations in Cells and Organisms* (ed. W. Wieser and E. Gnaiger), pp. 175–182. Stuttgart: Thieme.
- FULL, R. J. AND PRESTWICH, K. N. (1986). Anaerobic metabolism of walking and bouncing gaits in ghost crabs. *Am. Zool.* **26**, 88A.
- FULL, R. J. AND TU, M. S. (1990). Mechanics of six-legged runners. *J. exp. Biol.* **148**, 129–146.
- FULL, R. J. AND TU, M. S. (1991). Mechanics of rapid running insects: two-, four- and six-legged locomotion. *J. exp. Biol.* **156**, 215–231.
- FULL, R. J. AND WEINSTEIN, R. B. (1992). Integrating the physiology, mechanics and behavior of rapid running ghost crabs: slow and steady doesn't always win the race. *Am. Zool.* **32**, 382–395.
- GLÜCKLICH, D. (1976). Die Versteifung von Kunststoffmodellen durch elektrische Dehnungsmessstreifen. *VDI-Zeitschrift* **118**, 829–834.
- HEGLUND, N. C., CAVAGNA, G. A. AND TAYLOR, C. R. (1982). Energetics and mechanics of terrestrial locomotion. III. Energy changes of the centre of mass as a function of speed and body size in birds and mammals. *J. exp. Biol.* **79**, 41–56.
- HEGLUND, N. C., MCMAHON, T. A. AND TAYLOR, C. R. (1974). Scaling stride frequency and gait to animal size: mice to horses. *Science* **186**, 1112–1113.
- HEGLUND, N. C. AND TAYLOR, C. R. (1988). Speed, stride frequency and energy cost per stride: how do they change with body size and gait? *J. exp. Biol.* **138**, 301–318.
- HEPBURN, H. R. AND JOFFE, I. (1976). On the material properties of insect exoskeletons. In *The Insect Integument* (ed. H. R. Hepburn), pp. 107–235. Amsterdam: Elsevier.
- HILDEBRAND, M. (1980). The adaptive significance of tetrapod gait selection. *Am. Zool.* **20**, 255–267.
- HOYT, D. F. AND TAYLOR, C. R. (1981). Gait and the energetics of locomotion in horses. *Nature* **292**, 239–240.
- HUGHES, G. M. (1952). The co-ordination of insect movements. I. The walking movements of insects. *J. exp. Biol.* **29**, 267–284.
- LANYON, L. E. AND RUBIN, C. T. (1985). Functional adaptation in skeletal structures. In *Functional Vertebrate Morphology* (ed. M. Hildebrand, D. Bramble, K. F. Liem, D. B. Wake), pp. 1–23. Cambridge: Harvard University Press.

- MARSH, R. L. AND BENNETT, A. F. (1986). Thermal dependence of sprint performance of the lizard *Sceloporus occidentalis*. *J. exp. Biol.* **126**, 79–87.
- PERRY, A. K., BLICKHAN, R., BIEWENER, A. A., HEGLUND, N. C. AND TAYLOR, C. R. (1988). Preferred speeds in terrestrial locomotion: are they equivalent? *J. exp. Biol.* **137**, 207–209.
- RUBIN, C. T. AND LANYON, L. E. (1982). Limb mechanics as a function of speed and gait: a study of functional strains in the radius and tibia of horse and dog. *J. exp. Biol.* **101**, 187–211.
- SNYDER, R. C. (1962). Adaptations for bipedalism of lizards. *Am. Zool.* **2**, 191–203.
- SONG, S. M. (1984). Kinematic optimal design of a six-legged walking machine. PhD dissertation. Department of Electrical Engineering, Ohio State University.
- TAYLOR, C. R. (1978). Why change gait? Recruitment of muscles and muscle fibers as a function of speed and gait. *Am. Zool.* **18**, 153–161.
- TAYLOR, C. R. (1985). Force development during sustained locomotion: a determinant of gait, speed and metabolic power. *J. exp. Biol.* **115**, 253–262.